ROBUST QUANTUM MIXED STATE RECOVERY FROM AMPLITUDE DAMPING

A Thesis

by

SAEIDEH SHAHROKH ESFAHANI

Submitted to the Office of Graduate and Professional Studies of
Texas A&M University
in partial fulfillment of the requirements for the degree of

MASTER OF SCIENCE

Chair of Committee,	M. Suhail Zubairy
Committee Members,	Olga Kocharovskaya
	Alexei Sokolov
	Andreas Klappenecker
Head of Department,	George R. Welch

August 2016

Major Subject: Physics

ABSTRACT

Several instructions need to be considered in order to transfer classical error correction techniques to the quantum regime. The quantum error correction field has been developed to face these issues. One of the common source of errors in quantum systems is environment decoherence. Due to interaction with the environment, the quantum states of a system entangle with the environment and are subject to decoherence. In this thesis, we mainly focused on the amplitude damping which is one of the most important models of decoherence processes. We showed that general two-qubit mixed states undergoing an amplitude damping, can be almost completely restored using a reversal procedure. This reversal procedure through CNOT and Hadamard gates could also protect the entanglement of two-qubit mixed states from general amplitude damping. Concurrence and fidelity are two measurements used in order to examine how our proposed scheme performs. Furthermore, to give generality to our scheme, we proposed a robust recovery scheme to protect the quantum states when the decay parameters or the input quantum states are not completely known.

DEDICATION

To my beloved husband Mohammad

To my parents, Fatemeh and Ahmad

and

my sister Sepideh

ACKNOWLEDGEMENTS

First I would like to thank my parents, Fatemeh and Ahmad for all their loves and unconditional supports. Without them I would never have been able to achieve anything. Also, I would like to thank my sister, Sepideh who has always been my best friend from childhood and will be in the future.

I would like to thank my lovely husband, Mohammad for all of his support and professional guidance. His presence and persistent courage have helped me to find my very own way, and accelerating my endeavors in successfully finishing this thesis.

I would like to express my deepest gratitude to my advisor Prof. Zubairy, who made my thesis possible. I thank him for his steady guidance, inspirational discussions, and his dedication to high quality research through my master program at Texas A&M University. I would also like to thank Prof. Kocharovskaya, Prof. Sokolov and Prof. Klappenecker for serving on my committee and for their valuable comments and advice. I also would like to thank Dr. Zeyang Liao, for his advice and all his supports which helped me through this study.

I am sincerely thankful of Prof. Ricardo Eusebi by whom I started professional research in a graduate level at Texas A&M University. His supports and patience made my first experience as a researcher much easier and smoother.

Finally, I thank my friends Ansam Jameel Talib, Yusef Maleki and Sahar Delfan whose presence and helps have made the life easier and more joyful during my studies.

NOMENCLATURE

Qubit	Quantum Bit
DFS	Decoherence Free Subspace
QECC	Quantum Error Corection Code
CNOT gate	Controlled Not gate
Cavity QED	Cavity Quantum Electrodynamics
ESD point	Entanglement Sudden Death
RRS	Robust Recovery Scheme

TABLE OF CONTENTS

Page

ABSTRACT ii

DEDICATION iii

ACKNOWLEDGEMENTS iv

NOMENCLATURE v

TABLE OF CONTENTS vi

LIST OF FIGURES viii

LIST OF TABLES x

1. INTRODUCTION 1

    1.1 Measurement and reversal procedure 3
    1.2 Amplitude damping channel and weak measurement 3
        1.2.1 Amplitude damping reversal with monitoring the environment 5
        1.2.2 Uncollapsing a quantum state and the reversal measurement . 6
        1.2.3 Reversal measurement with quantum gates 7
        1.2.4 Thesis contribution 8

2. QUANTUM STATE RECOVERY UNDERGOES AMPLITUDE DAMPING 10

    2.1 Amplitude damping of two-qubit mixed state 10
        2.1.1 Two-qubit mixed states recovery 12
    2.2 Protect from the entaglement 14
        2.2.1 Fidelity 14
        2.2.2 Concurrence 17
    2.3 Extended scheme 18

3. ROBUST RECOVERY SCHEME 25

    3.1 Robust recovery under uncertainty 25
        3.1.1 Uncertainty in p 25
        3.1.2 Unknown p and ρ 28
        3.1.3 Simulation 29

4. CONCLUSION 32

REFERENCES 33

LIST OF FIGURES

FIGURE Page

1.1 A schematic view of the two level atom placed in vacuum undergoes spontaneous emission (left) and a field state inside a leaky cavity(right) 2

1.2 A schematic view of the uncollapsing sequence suppressing energy relaxation n a phase qubit in [15]. 6

1.3 Circuit diagram for the reversal of the weak measurement of one qubit in [17]. 7

1.4 Circuit diagram for the reversal of theamplitud damping of two qubit pure state in [18]. 8

1.5 Schematic workflow coresponds to the thesis contributions. 9

2.1 A schematic view of the recovery process proposed in [18], generalized herein for the mixed states setting. 11

2.2 F_d (dashed line) and F_r (solid line) as a function of decaying factor p. Panels (a) and (b) show the results for $\rho 1$ and $\rho 2$ described in Eq.(2.13), respectively. 16

2.3 The average fidelity of the damped and recovered states via Monte Carlo method with 10^4 iteration as a function of damping probability (p) 17

2.4 Concurrence as a function of damping probability, p, for damped state and recovered state. Corresponding to ρ_1 and ρ_2 described in Eq. (2.13) respectively. 21

2.5 A schematic view of the extended scheme process proposed in [18], generalized herein for the mixed states setting. 22

2.6 Concurrence as a function of damping probability for damped state and recovered state corresponds to the results in Section 2.2.2 and the other curves relates to $x = 0.1$, $x = 0.5$ and $x = 0.8$. All curves are belonging to ρ_1 and ρ_2 described in Eq. (2.13). 23

2.7 Fidelity in the extended scenario as a function of damping probability. Damped state and recovered state corresponds to the results in Section 2.2.1. The other curves relates to $x = 0.1$, $x = 0.5$ and $x = 0.8$ in the extended scenario. All curves are belonging to ρ_1 and ρ_2 described in Eq. (2.13). 24

3.1 The system states are ρ_1 and ρ_2. The solid line and dashed line depends on fidelity with known p and adaptive θ with p, ($\theta = \tan^{-1}(1/\sqrt{1-p})$, used in 2.2.1. The doted line depends on fixed θ which obtains from $\theta = \tan^{-1}(1/\sqrt{0.3})$. 27

3.2 The illustrative scheme of Monte Carlo simulations. 30

LIST OF TABLES

TABLE Page

2.1 CNOT gates used for recovery in Fig. 2.1 12

3.1 Average recovery fidelity for two scenarios. The first row shows the results for the case where p and ρ are assumed unknown. Also the results are repeated periodically until 2π. The second row show the fidelity for the scenario where the gate angle is chosen with the knowledge of p same as Sec. 2.2.1. The third row is the average damped fidelity. 29

3.2 Average recovery fidelity for two scenarios. p varied from 0.40 to 0.60. The first row shows the results for the RRS scheme. The second row show the fidelity for the scenario where the gate angle is chosen with the knowledge of p same as Sec. 2.2.1. The third row is the average damped fidelity. 31

3.3 Average recovery fidelity for two scenarios. p varied from 0.45 to 0.55. The first row shows the results for the RRS scheme. The second row shows the fidelity for the scenario where the gate angle is chosen with the knowledge of p same as Sec. 2.2.1. The third row is the average damped fidelity. 31

1. INTRODUCTION

Due to the inevitable interaction with the environment, a quantum system can entangle with the environment and subsequently becomes *decoherent*. This decoherence procedure is a fundamental obstacle for successful transfer of quantum information and for practical quantum computation. A number of effective approaches have been proposed to suppress the decoherence effect. One way for protecting a quantum state from decoherence is based on the existence of decoherence free subspaces (DFS) which requires special symmetry properties of the interaction Hamiltonian. In Quantum Computation, this procedure, i.e. utilization of DFS to protecting quantum states, is called "error-avoiding code" [1]. "Quantum error correction code (QECC)" is another way to suppress the decoherence effect. In QECC, the logical quantum bit (qubit) is encoded in a larger Hilbert space of several physical qubits and the correction process is performed by constructing proper measurements and correction operations [2, 3]. Other methods such as quantum Zeno effect [4, 5] and dynamical decoupling [6, 7] are also widely used to mitigate decoherence and to protect the quantum state.

Amplitude damping is a consequence of the coupling of the system with a reservior and therefore it is a fundumental source of noise in many syestems [8]. For exampale, an atom placed in vacuum can undergo spontaneous emission. Similarly, a field state inside a leaky cavity can intercat with vacuum modes outside the cavity and consequently loss its coherence, schematicly shown in FIg. 1.1. In the past years, several strategies have been proposed to protect quantum states from the amplitude damping. Three widely used strategies to protect the quantum state from amplitude damping are: (1) weak measurement reversal [12, 13, 14, 15], (2) un-collapsing a quantum state towards the ground state and the reversal measurement [16], and (3)

Figure 1.1: A schematic view of the two level atom placed in vacuum undergoes spontaneous emission (left) and a field state inside a leaky cavity(right)

utilization of quantum gates to restore a qubit state in a weak measurement [17, 18]. Quantum state recovery based on quantum gates can be implemented in a shorter time compared with the weak measurement reversal. It is shown that a one-qubit state in a weak measurement can be completely recovered by applying Hadamard and CNOT gates on the system qubit and an auxiliary qubit [17]. This method is generalized to recover an arbitrary two-qubit pure state undergoing amplitude damping [18].

In this thesis, we show that this method can be generalized to protect an arbitrary two-qubit mixed states which can have many more free parameters as compared to a pure superposition state. We also consider the case when the input density matrix and the damping parameter are not completely known (or partially known) and propose a robust recovery scheme. We test our recovery schemes by generating arbitrary mixed states via Monte-Carlo simulations and obtain the optimal parameters to recover an unknown quantum state. Here, we restrict our analysis to zero temperature, as we are only interested in reversing the noise due to quantum fluctuation.

This chapter provides a motivation and general introduction to reversal procedures of a quantum state from amplitude damping.

1.1 Measurement and reversal procedure

Quantum measurement is located at the heart of controversial discussion of quantum mechanics. A quantum state is defined as a superposition of the eigenstates of the system. The main issue occurs when the system collapses because of the act of measurement given an eigenvalue corresponding to an eigenstate [2]. Thus, the crucial question here is that "would it be possible to reverse a measurement and recover the original state?" Traditionaly the answer was no. Due to collapsing of wave function, the original state is gone forever. However, as this thesis will discuss in the following chapters, there is a class of measurements so called "weak measurement", which can restore any unknown premeasured state, though with the probability less than unity [14, 13]. In the weak measurement, full information of the probability amplitude is retained in the superposition of the states. So, in other words, the more strong measrement, the less probability of successful recovery.

1.2 Amplitude damping channel and weak measurement

Envoironmental decoherence is one important source of errors in quantum systems. In order to model this decoherence, in this thesis, we consider amplitude damping which can be a field in a leaky cavity, two level atom with spontaneous emission, etc. A single qubit amplitude damping can be mathematically described by the following mappings:

$$\begin{aligned} |0\rangle_S|0\rangle_E &\rightarrow |0\rangle_S|0\rangle_E \\ |1\rangle_S|0\rangle_E &\rightarrow \sqrt{1-p}|1\rangle_S|0\rangle_E + \sqrt{p}|0\rangle_S|1\rangle_E \end{aligned} \tag{1.1}$$

where $p \in [0, 1]$ is the possibility of decaying of the excited state, and S (E) denotes the system (environment). For exapmle, within the Weisskopf-Wigner approximation

[8], the decaying probability of an atom interacting with vacuum field is given by $\sqrt{1-p} = e^{-\Gamma t}$ with Γ being the spontaneous decay rate of an atom. Similarly, the damping of a field in a cavity is given by $\sqrt{1-p} = e^{-\kappa t}$ with κ being the leakage rate of a cavity.

Let us consider a two level atom with spontaneous emission and suppose that an ideal detector is placed outside of the system in the environment [9]. If the detector detects a photon, it seems that we have prepared $|0\rangle_E$. In fact we know with certainty that the initial state was the excited state, because the ground state could not have decayed. On the other hand, if we detect no photon with our ideal detector then we have projected out the state $|0\rangle_E$ of the environment. Therefore, we have prepared the atomic state: $a\,|0\rangle_A + b\,|1\rangle_A$.

As we saw, the atomic state was obtained due to our failure to detect a photon. This is an example of a "weak measurement" where we obtain partial information about the state but the information about the amplitude a and b can be fully recovered. In contrary, if ther is no detector in the environment we have:

$$(a\,|0\rangle_A + b\,|1\rangle_A\,|0\rangle_E = (a|0\rangle_A + b\sqrt{1-p}\,|1\rangle_A)|0\rangle_E + \sqrt{p}|0\rangle_A|1\rangle_E \tag{1.2}$$

In this thesis, we aime to present new schems in order to recover the initial state from amplitude damping in Eq 1.2 and show that even without weak measurement, quantum entanglement of a two-qubit system can also be partially protected using the proposed schemes.

In the following, we will begin with three widely used strategies to protect the quantum state from amplitude damping in the weak measurement and after that we will discuss about our schem for recovery without weak measurement.

1.2.1 Amplitude damping reversal with monitoring the environment

As we discussed in the previous section, using weak measurment would be beneficial in order to recover the initial state from amplitude damping.

In [13], the authors demonstrated the probabilistic reversal procedure with continuos weak measurement applied to solid-state qubits. At the first step, [13] consideres a quantum double dot qubit, measured by a quantum point contact. The authors practically described how to undo the measurement and calculate its related probability, as well as the mean undoing time. At the second step, they demonstrated the same procedure similar to the first step for the phase qubit. The general theory of the reversal measurement proposed in this paper is that they described a linear operator M_r for general measurement with result called r. Thus, for an initial state the ρ probability of the result r is $P_r(\rho) = Tr(E_r\rho)$ where $E_r = M_r^\dagger M_r$ which is a positive Hermitian operator. The state after measurement changes to $\rho = M_r\rho M_r^\dagger / Tr(E_r\rho)$. In order to reverse the measurement, they applied the inverse operation characterized by $L_r = CM_r^{-1}$ where C is a complex number. Since L_r can be physical only if all eigenvalues of $L_r^\dagger L_r$ are ≤ 1, it leads to conclude the upper limit bound $|C|^2 \leq \ min_i P_i$, where $\{P_i\}$ is the set of eigenvalues of E_r. Therefore, the probability of success $P_s = Tr\left(L_r^\dagger L_r \tilde{\rho}\right)$ corresponding to L_r is bounded by ${}^{min_i P_i}/_{P_r(\rho)}$. Finally, it is concluded that the upper bound for the successful reversal measurement probability, similar to [7], is $P_s \leq {}^{(minP_r)}/_{P_r\rho}$. They compare the probability results found for the two considered systems where proof that results of two systems reach the defined upper bound P_s.

Furthermore, Sun et. al in [14], proposed that by using weak measurement, we can reverse the entanglement change of two qubits. They assumed that two entangled qubits interacted with their own individual environments due to undergoing different

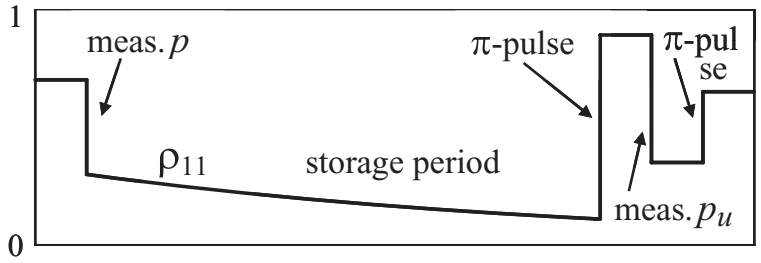

Figure 1.2: A schematic view of the uncollapsing sequence suppressing energy relaxation n a phase qubit in [15].

paths. Gradually, their entanglement became changed. To recover the entanglement they first apply bit flip operation to both qubit, then perform a null-result weak measurement, and finally flip the qubits back. Finally, paper concludes that the initial entangled state and the entanglement were recovered exactly due to using weak measurement.

1.2.2 Uncollapsing a quantum state and the reversal measurement

As another approach of reversal measurement, [15] used scheme introduced in Fig. 1.2 They started with moving the qubit state toward the ground state in a coherent but non unitary way (as in Ref. [11]) to protect the qubit against zero-temperature energy relaxation.

Then after the storage time they apply the uncollapsing procedure for the phase qubit consisting of a pulse, second partial measurement, and one more π pulse which restores the initial qubit state. The procedure was probabilistic since specific result of both measurements were selected. The measurement was rejected at the selection of the second measurement, if an energy relaxation event happens during the storage period. Therefore, in the first step and to analyze the procedure quantitatively, they

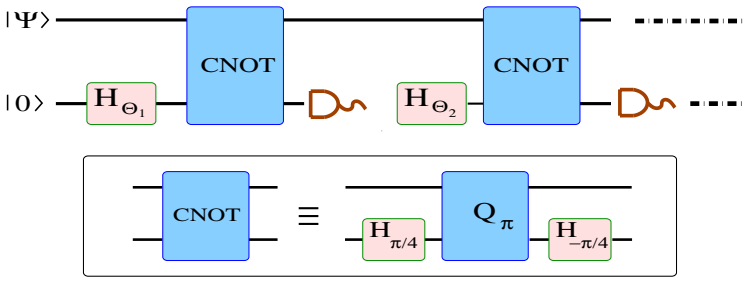

Figure 1.3: Circuit diagram for the reversal of the weak measurement of one qubit in [17].

considered the initial state of the qubit within a rotating frame. After applying the reversal procedure they characterized the performance of the proposed scheme by calculating fidelity of the quantum state storage. Then, after some calculation, they concluded that the uncollapsing is the only known method of improving the qubit storage fidelity against energy relaxation.

1.2.3 Reversal measurement with quantum gates

In 2011 Al Amri et al. [17] suggested to directly choose ancilla qubit following with appropriate quantum gates for reversal procedure. They proposed the circuit diagram depicted in Fig. 1.3 for the reversal of the weak measurement of one qubit pure state undergone amplitude damping. The advantage of their proposed scheme include iterativiity iterative and experimentally being realizable within the presently available cavity quantum eloctrodynamics (QED) systems. Furthermore, although no weak measurement required and the reversal state was accomplished in a small time in the reversal process, the probability of success remained essentially the same. After that, in [18], Liao et al. extended the scheme in Fig. 1.3 for reversing of tow qubit pure state and proposed the scheme described in Fig. 1.4 for that.

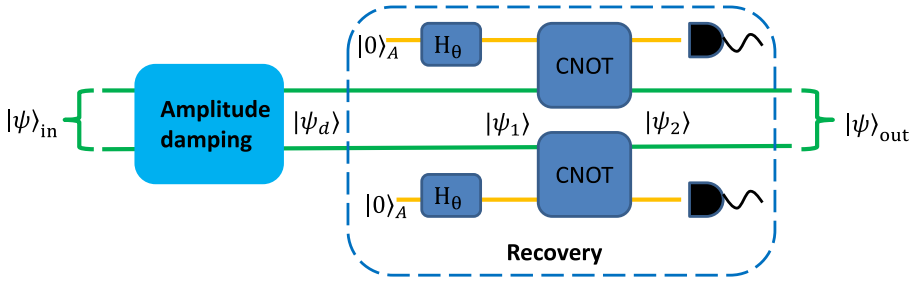

Figure 1.4: Circuit diagram for the reversal of theamplitud damping of two qubit pure state in [18].

1.2.4 Thesis contribution

All approaches mentioned above, were recovering the damped quantum state by employing weak measurements. So, the question becomes "what if we aim to recover the quantum state in general amplitude damping meaning that in this situation there is no weak measurement?" In second part of the paper [18], Ziao et al. show that using similar procedure in Fig. 1.3, two qubit pure state could be recovered when system was undergoes general amplitude damping. The work presented in this thesis aims to further expande the applicability of the proposed circuit in Figs. 1.3 and 1.4, by considering it within two-qubit mixed state framework and discuss how a robust scheme can revover the amplitude damping once we have uncertainty in the underlying quantum system. The schematic workflow of thesis contributions is depicted in fig. 1.5.

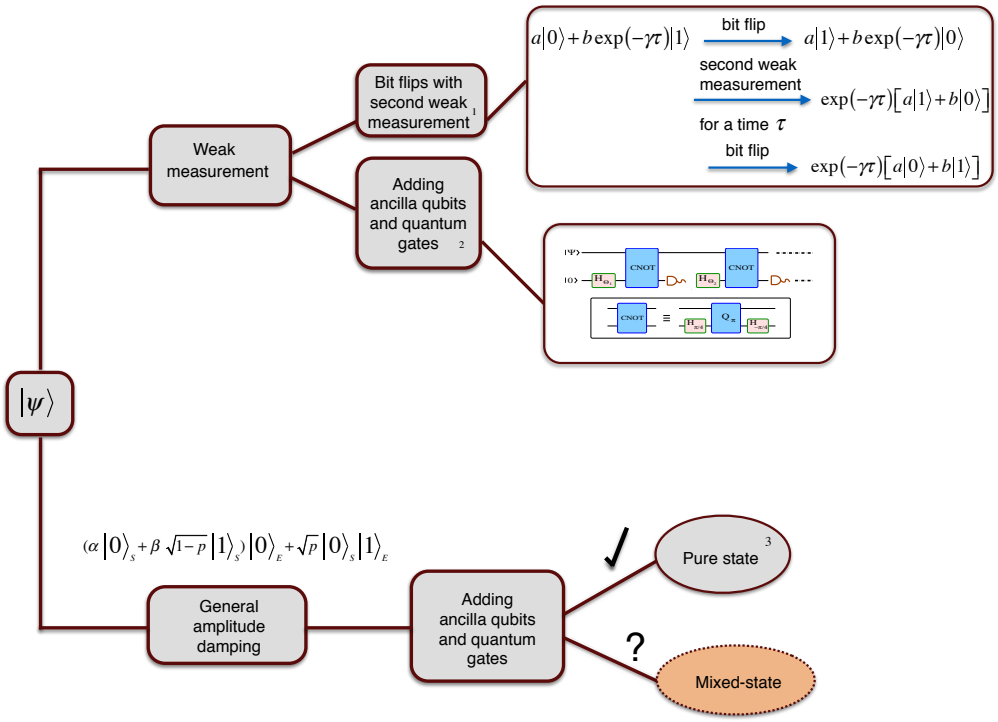

1. Sun Q, Al-Amri M, Davidovich L and Zubairy M. S. 2010 *Phys. Rev.* A 82 052323
2. Al Amri, Scully, Zubairy, J. Phys. B: At. Mol. Opt. Phys. 2011, 44 (2011) 165509
3. Liao, Al Amri, Zubairy, J. Phys. B: At. Mol. Opt. Phys. 2013, 46 (2013) 145501

Figure 1.5: Schematic workflow coresponds to the thesis contributions.

2. QUANTUM STATE RECOVERY UNDERGOES AMPLITUDE DAMPING

Consider amplitude damping in order to model the environmental decoherence of a quantum system. Since we aime to work in the mixed-state framework, in this chapter, we begin with amplitude damping of two-qubit mixed-state. Then, the initial state is recovered by schemes proposed in this thesis.

2.1 Amplitude damping of two-qubit mixed state

Following the universal chracter of amplitude damping explained in introduction, it is appropriate to begin the amplitude damping within the mixed-state frame work. The amplitude damping operations are given by [10].

$$A_0 = \begin{pmatrix} 1 & 0 \\ 0 & \sqrt{1-p} \end{pmatrix}, A_1 = \begin{pmatrix} 0 & \sqrt{p} \\ 0 & 0 \end{pmatrix}. \tag{2.1}$$

An arbitrary two-qubit mixed state can be written as

$$\rho_i = \begin{pmatrix} a & e & f & g \\ e^* & b & h & i \\ f^* & h^* & c & j \\ g^* & i^* & j^* & d \end{pmatrix}. \tag{2.2}$$

The amplitude damping of an arbitrary two-qubit mixed state can be calculated by the following procedures. First an arbitrary two-qubit mixed state can be also written as $\rho = \sum_{i,j,m,n=0}^{1} \alpha_{ijmn} |ij\rangle\langle mn|$. Each element $|ij\rangle\langle mn\rangle$ can be written as two-qubit direct products $|i\rangle\langle m| \otimes |j\rangle\langle n|$. Next we apply the amplitude damping

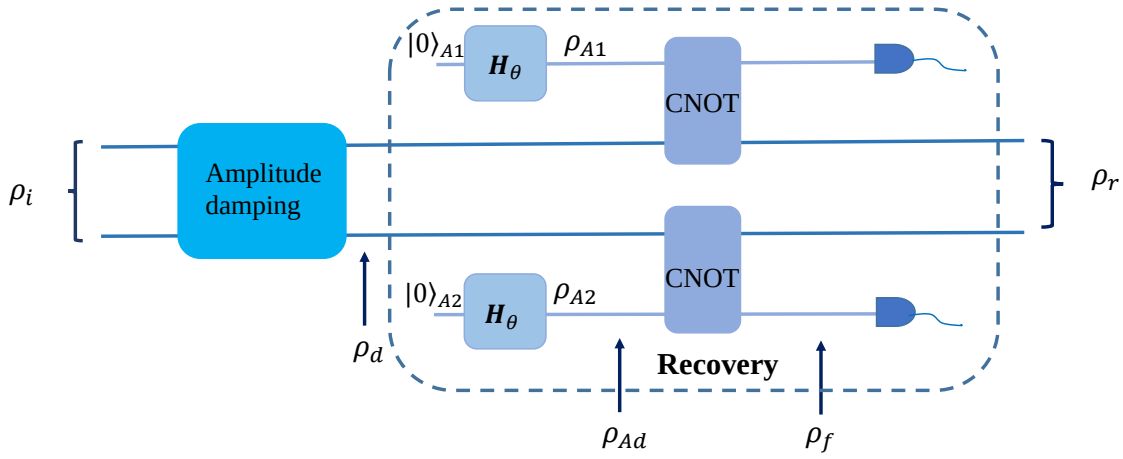

Figure 2.1: A schematic view of the recovery process proposed in [18], generalized herein for the mixed states setting.

operations on each qubit which yields

$$|ij\rangle\langle mn| \to \left[A_0 |i\rangle \langle m| A_0^\dagger + A_1 |i\rangle \langle m| A_1^\dagger\right] \bigotimes \left[A_0 |j\rangle \langle n| A_0^\dagger + A_1 |j\rangle \langle n| A_1^\dagger\right]. \quad (2.3)$$

After applying the amplitude damping operations on each element, we obtain the two-qubit amplitude damped state given by

$$\rho_d = \begin{pmatrix} a + bp + cp + p^2 d & e\sqrt{q} + pj\sqrt{q} & f\sqrt{q} + ip\sqrt{q} & gq \\ e^*\sqrt{q} + pj^*\sqrt{q} & bq + pdq & hq & iq\sqrt{q} \\ f^*\sqrt{q} + i^*p\sqrt{q} & h^*q & cq + pdq & jq\sqrt{q} \\ g^*q & i^*q\sqrt{q} & j^*q\sqrt{q} & dq^2 \end{pmatrix}. \quad (2.4)$$

where $q = 1 - p$.

2.1.1 Two-qubit mixed states recovery

In this section, we propose a method to recover the damped quantum mixed states in Eq. (2.4) to the initial quantum mixed states in Eq. (2.2). This method has recently been introduced for two-qubit pure state [18]. In this model, we use the circuit diagram outlined in Fig. 2.1. Two auxiliary qubits both in the $|0\rangle$ state initially, are added. First, we apply a Hadamard gate with angle θ for each ancilla qubit.

$$H_\theta = \begin{pmatrix} \cos\theta & -\sin\theta \\ \sin\theta & \cos\theta \end{pmatrix} \tag{2.5}$$

The ancilla qubits ($A1$ and $A2$) after passing through the Hadamard gate will change to:

$$\rho_{A1} = \rho_{A2} = \begin{pmatrix} \cos\theta^2 & \cos\theta\sin\theta \\ \cos\theta\sin\theta & \sin\theta^2 \end{pmatrix}. \tag{2.6}$$

The state of the whole system, after combining ancilla qubits to the damped system in Eq. (2.4) can be written as:

$$\rho_{Ad} = \rho_{A1} \bigotimes \rho_d \bigotimes \rho_{A2}. \tag{2.7}$$

Afterwards, we apply two CNOT gates onto each pair of the system and ancilla qubits: The final state is then given by:

CNOT gate I	CNOT gate II
$UC_1 = \begin{pmatrix} 1 & 0 & 0 & 0 \\ 0 & 0 & 0 & 1 \\ 0 & 0 & 1 & 0 \\ 0 & 1 & 0 & 0 \end{pmatrix}$	$UC_2 = \begin{pmatrix} 1 & 0 & 0 & 0 \\ 0 & 1 & 0 & 0 \\ 0 & 0 & 0 & 1 \\ 0 & 0 & 1 & 0 \end{pmatrix}$

Table 2.1: CNOT gates used for recovery in Fig. 2.1

$$\rho_f = UC_1 \bigotimes UC_2 \cdot \rho_{Ad} \cdot {UC_2}^\dagger \bigotimes {UC_1}^\dagger \tag{2.8}$$

Finally, we make measurements on the two ancilla qubits. If the ancilla qubits are both in $|0\rangle$ state, the recover process is successful. Otherwise, the recover process fails. Since the ancilla qubits are measured to be in $|0\rangle$ state, the state of the whole system becomes

$$\rho_f^{'} = (P_{A1} \otimes P_{A2}) \rho_f (P_{A2}^\dagger \otimes P_{A1}^\dagger) \tag{2.9}$$

where the projection operators $P_{A1} = |0\rangle\langle 0| \bigotimes \mathbb{I}_2$ and $P_{A2} = \mathbb{I}_2 \bigotimes |0\rangle\langle 0|$ with $\mathbb{I}_2$ being a two-by-two unit matrix. The reduced system density matrix is $\rho_r = Tr_{A1,A2}(\rho_{f1}^{'})$ where $Tr_{A1,A2}$ denotes the partial trace over the ancilla qubits.

By choosing $\theta = \tan^{-1}(1/\sqrt{q})$, the final state after the recovery process for the system can be calculated to be

$$\rho_r = \frac{1}{1+(1-a+d)p+p^2 d} \begin{pmatrix} a+bp+cp+p^2 d & e+pj & f+ip & g \\ e^*+j^*p & b+pd & h & i \\ f^*+i^*p & h^* & c+pd & j \\ g^* & i^* & j^* & d \end{pmatrix}. \tag{2.10}$$

From Eq. 2.10 we can obtain $\rho_r = (\rho_i + \rho_{err})/N$ where ρ_i is the initial state, $N = 1+(1-a+d)p+p^2 d$ is the normalization factor, and ρ_{err} the recovering error matrix which is given by

$$\rho_{err} = \begin{pmatrix} bp+cp+p^2 d & jp & ip & 0 \\ j^*p & dp & 0 & 0 \\ i^*p & 0 & pd & 0 \\ 0 & 0 & 0 & 0 \end{pmatrix}. \tag{2.11}$$

Thus, the system is not completely recovered but is restored to the initial input

density matrix plus an error term. When $p = 0$, $\rho_r = \rho_i$ which is expected. Here, we have neglected the amplitude damping of the system qubits and ancilla qubit during the recovery process. This is a good approximation as the recovery process is based on quantum gates which can be implemented much faster than the decoherence time of the system. For example, a CNOT gate can be implemented by a cavity-QED system proposed by [17] where the interaction time is around $20\mu s$ while the atom and field relaxation time are $30ms$ and $1ms$, respectively [19]. In the following, we quantitatively analyze how the quantum state is restored using fidelity and quantum concurrence

2.2 Protect from the entaglement

The entanglement is the phenomenon related to non separable states whereby particles interacting with each other become permanently dependent to each other. In this situation they act as a single entity. Variety of measurements, such as entanglement cost, entropy measurement, concurrence and fidelity, are used to quantify the entanglement. In this thesis, fidelity and concurrence are considered for measuring the entanglement of states.

2.2.1 Fidelity

In quantum information theory, fidelity is a quantity which is determine how two states are distinguishable. Therefore, in order to study how a quantum state is recovered with proposed scheme, we calculate the fidelity between the recovered and the initial states. The fidelity function between two quantum mixed states is defined by [20]

$$F(\rho_i, \rho_f) = \left[Tr\left(\sqrt{\sqrt{\rho_i}\rho_f\sqrt{\rho_i}} \right) \right]^2, \tag{2.12}$$

where ρ_i and ρ_f are the initial and final state, respectively. In this study, the fidelity between the damped state and the initial state is $F_d = F(\rho_i, \rho_d)$, and the fidelity between the recovered state and the initial state is $F_r = F(\rho_i, \rho_r)$.

In Figs. 2.2(a) and 2.2(b), we depict the recovering fidelities as a function of the decaying probability p for two mixed states given by:

$$\rho_1 = \begin{pmatrix} 0.4 & 0 & 0 & 0.25 \\ 0 & 0.1 & 0 & 0 \\ 0 & 0 & 0.3 & 0 \\ 0.25 & 0 & 0 & 0.2 \end{pmatrix}, \ \rho_2 = \begin{pmatrix} 0.6 & 0 & 0 & 0.25 \\ 0 & 0.12 & 0 & 0 \\ 0 & 0 & 0.11 & 0 \\ 0.25 & 0 & 0 & 0.17 \end{pmatrix} \tag{2.13}$$

From the figures, we see that the fidelities of the recovered states are higher than those of the damped states which indicates that our recovery scheme also works for the two-qubit mixed states.

To justify whether our method works for general two-qubit mixed states, we also perform the numerical calculation of average fidelity of the damped states and the recovered states over a large ensemble. To do so, we randomly generate a large ensemble of two-qubit mixed state using the method shown in [21, 22, 23] in which they would obey the required properties of a valid density matrix from a certain probability distribution. Following [22], for generating an ensemble of random density matrices, we firs generated a Ginibre ensemble and then used the probability measure induced by the Bures metric. After that, for each decaying probability p, θ is chosen to be $tan^{-1}(1/\sqrt{1-p})$ and the average fidelity of the damped and recovered states are shown in Fig. 2.3 where we can see that our recovery scheme can effectively restore the general two-qubit mixed state.

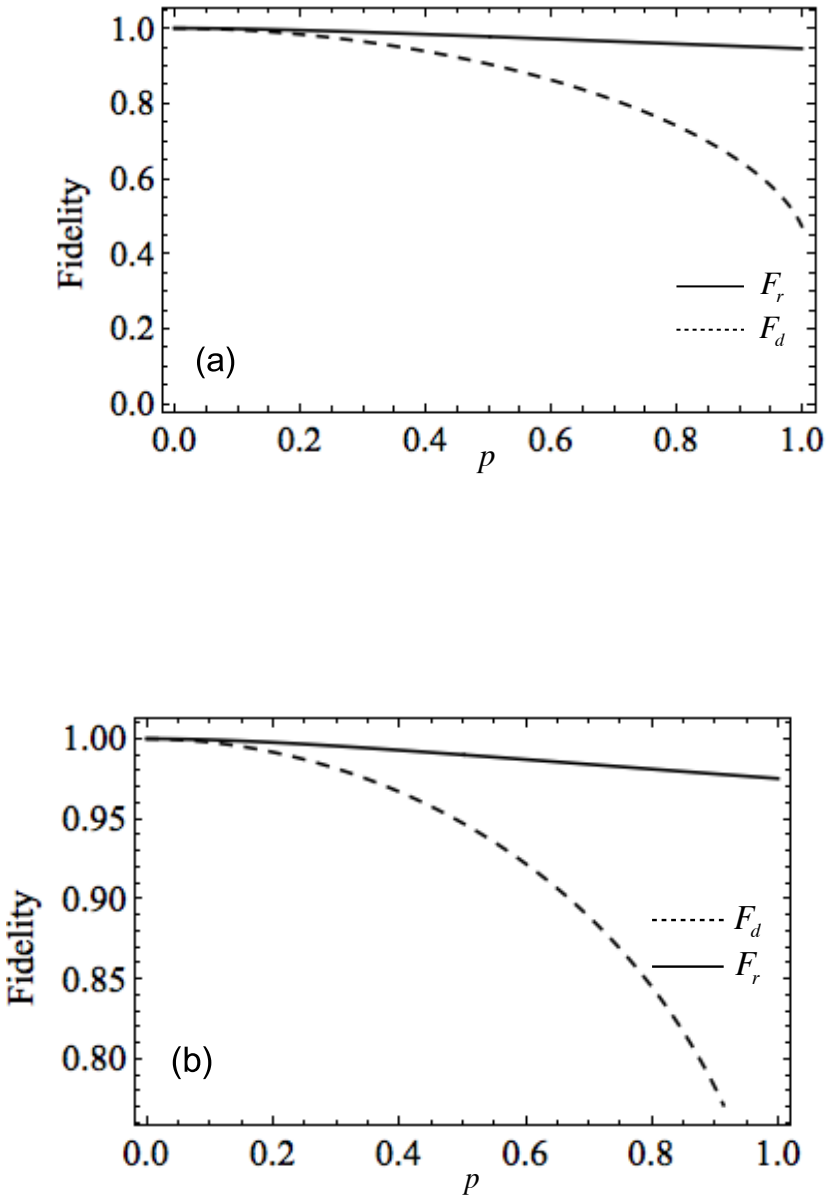

Figure 2.2: F_d (dashed line) and F_r (solid line) as a function of decaying factor p. Panels (a) and (b) show the results for $\rho 1$ and $\rho 2$ described in Eq.(2.13), respectively.

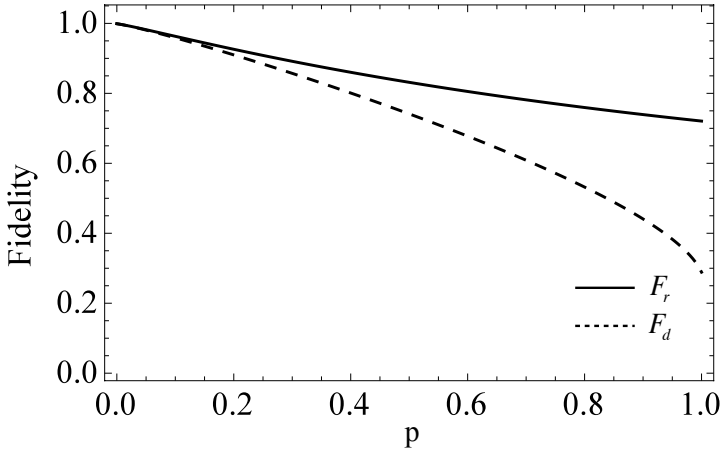

Figure 2.3: The average fidelity of the damped and recovered states via Monte Carlo method with 10^4 iteration as a function of damping probability (p)

2.2.2 Concurrence

In this subsection, we study whether the quantum entanglement of the two-qubit mixed state can be protected by our scheme or not. The quantum entanglement of a two-qubit mixed state can be calibrated by the quantum *"concurrence"* which is defined as [24]

$$C(\rho) \equiv \max\left(0, \lambda_1 - \lambda_2 - \lambda_3 - \lambda_4\right), \tag{2.14}$$

in which $\lambda_1, ..., \lambda_4$ are the eigenvalues in decreasing order of the Hermitian matrix $R(\rho) = \sqrt{\sqrt{\rho}\tilde{\rho}\sqrt{\rho}}$ with $\tilde{\rho} = (\sigma_y \bigotimes \sigma_y)\rho^*(\sigma_y \bigotimes \sigma_y)$.

The damped concurrence and the recovered concurrences for the two quantum states used in the previous section are shown in Fig. 2.4(a) and 2.4(b) respectively. From Figs. 2.4(a) and 2.4(b) one can see the following features: (1) The concurrence of recovered state is higher than that of the damped one which indicates that our scheme can protect the quantum entanglement of the two-qubit mixed state from

amplitude damping. However, the amount of the quantum entanglement does not improve very much. (2) The entanglement vanishes at a special point which is called *entanglement sudden death* (ESD) [25, 26]. Before the ESD point, the quantum entanglement can be restored by a certain amount. However, beyond the ESD point, the quantum entanglement can not be improved by the quantum algorithm shown in Fig. 2.1 because the recovering scheme shown in Fig. 1 is essentially non-unitary local operation.

2.3 Extended scheme

In the previous section, we show that a quantum state can be recovered with very good fidelity by the scheme shown in Fig. 1. However, the quantum entanglement can not be well recovered in that scheme. In this section, we discuss how to improve this scheme. Similar to that of [18], we can significantly improve the fidelity and quantum entanglement by adding a preparation stage before the amplitude damping of a two-qubit mixed state. The extended scheme scenario is depicted in Fig. 2.5, which is a mixed-state generalization of the scheme in [18].

The proposed method proceeds as follows: Before the initial two-qubit mixed states undergoes amplitude damping, we pre-process the system to make it robust against the amplitude damping. To do so, we apply the same quantum circuit as in the recovery part to *prepare* the initial state. In this stage, the preparation is successful if the ancilla qubits are measured to be $|00\rangle$. After the preparation stage, the system undergoes the damping stage shown in Sec. 2.1. In the final part, we perform the same recovery procedure as shown in Sec. 2.1.1 to recover the quantum state and quantum entanglement.

The quantum state after the preparation stage can be obtained from Eq. (2.10), by considering $p = 0$ and $\theta = \theta_1$ where θ_1 is the rotation angle of Hadamard gate

in the preparation step. Then, by denoting $x \equiv \tan^2\theta_1$, the quantum state after the preparation stage is given by

$$\rho_p = \begin{pmatrix} \frac{a}{(1+x)^2} & e(\frac{1}{1+x})^{3/2}\sqrt{\frac{x}{1+x}} & f(\frac{1}{1+x})^{3/2}\sqrt{\frac{x}{1+x}} & \frac{gx}{(1+x)^2} \\ e^*(\frac{1}{1+x})^{3/2}\sqrt{\frac{x}{1+x}} & \frac{bx}{(1+x)^2} & \frac{hx}{(1+x)^2} & i(\frac{1}{1+x})^{3/2}\sqrt{\frac{x}{1+x}} \\ f^*(\frac{1}{1+x})^{3/2}\sqrt{\frac{x}{1+x}} & \frac{h^*x}{(1+x)^2} & \frac{cx}{(1+x)^2} & j(\frac{1}{1+x})^{3/2}\sqrt{\frac{x}{1+x}} \\ \frac{g^*x}{(1+x)^2} & i^*(\frac{1}{1+x})^{3/2}\sqrt{\frac{x}{1+x}} & j^*(\frac{1}{1+x})^{3/2}\sqrt{\frac{x}{1+x}} & \frac{dx^2}{(1+x)^2} \end{pmatrix}. \tag{2.15}$$

It is noted that if θ_1 is selected such that $x < 1$, the system uncollapses toward the ground state as weak measurement [16, 15]. The ground state is less vulnerable to the amplitude damping because it is uncoupled to the environment [16]. In the next stage, the prepared state shown in Eq. (2.15) undergoes the amplitude damping and the recovery procedure, shown in Fig 2.5. For the recovery stage we determine the rotation angle of the Hadamard gate, θ_2, such that $xqy = 1$ where $y \equiv \tan^2\theta_2$. Then, as in Sec. 2.1.1, we measure the ancilla qubits in $|00\rangle$ states, and finally obtain the recovered density matrix.

We now examine how our extended scheme works compared with the scheme without preparation stage. In Figs. 2.6(a) and 2.6(b), we show the quantum entanglement recovery C_r under different values of x. From the figures, we see that C_r in the extended scheme with $x < 1$ can be higher than C_r in the previous scheme without preparation stage. When $x = 1$, C_r in the extended scheme returns back to the previous one. In addition, we notice that the quantum entanglement does not vanish in the extended scheme even beyond the ESD point which never occur in the previous scheme. The reason why the ESD can be inhibited in the extended scheme is because we prepare the initial state in a more robust state by un-collapsing the quantum state toward the ground state before the amplitude damping. The more

we un-collapse the system toward the ground state, the larger the ESD point will be. After a certain value, the ESD point can be even eliminated in the whole region. The fidelity of the recovered state can be also significantly improved in the extended scheme (see Figs. 2.7(a) and 2.7(b)). However, we note that the success probability decreases when x is smaller.

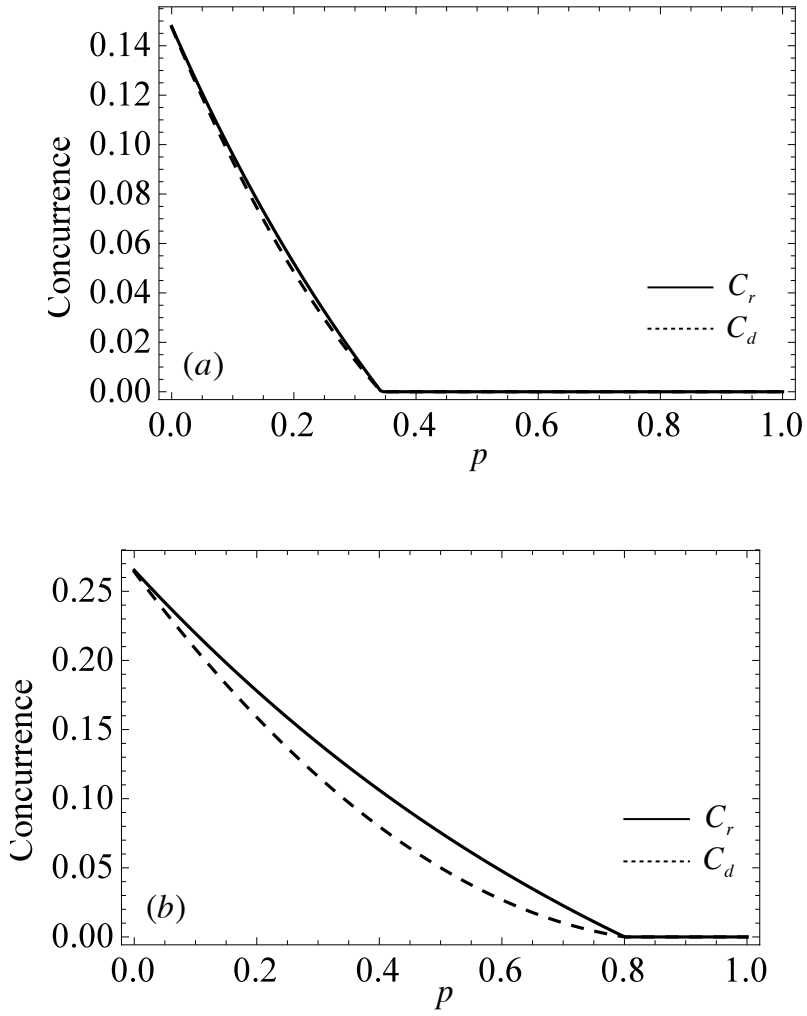

Figure 2.4: Concurrence as a function of damping probability, p, for damped state and recovered state. Corresponding to ρ_1 and ρ_2 described in Eq. (2.13) respectively.

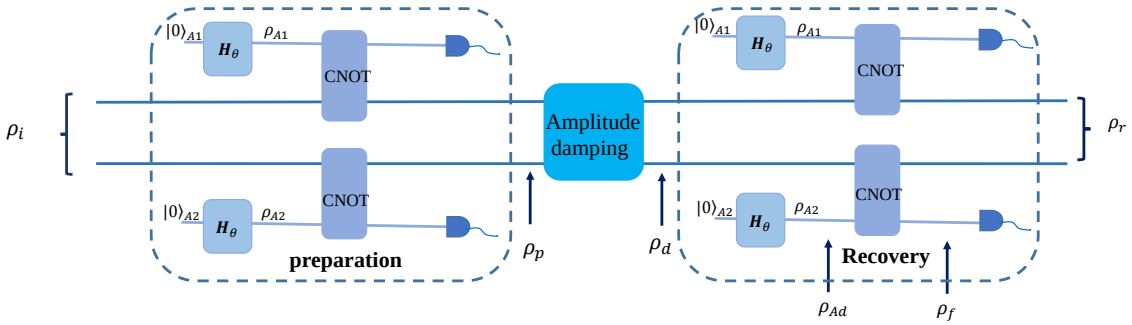

Figure 2.5: A schematic view of the extended scheme process proposed in [18], generalized herein for the mixed states setting.

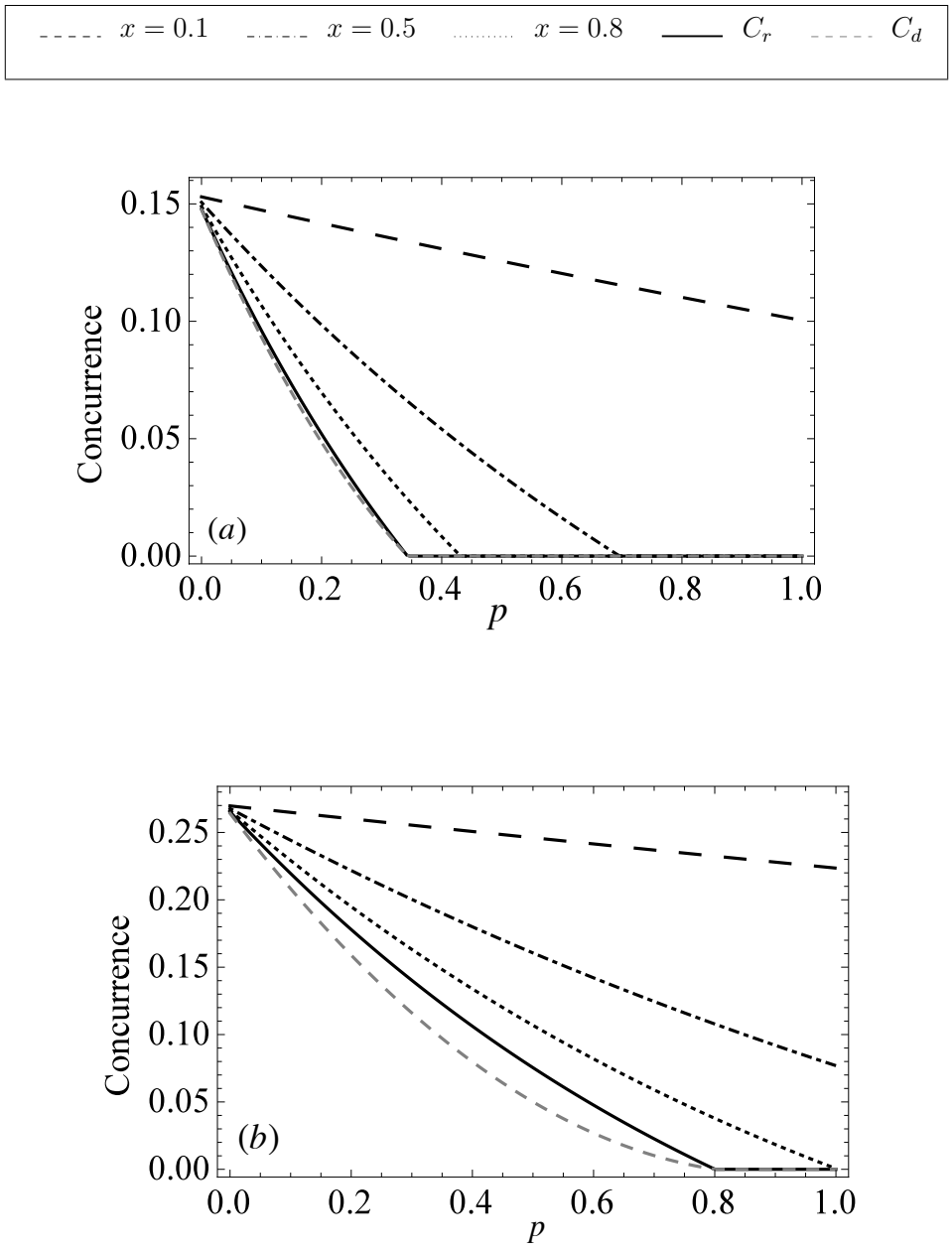

Figure 2.6: Concurrence as a function of damping probability for damped state and recovered state corresponds to the results in Section 2.2.2 and the other curves relates to $x = 0.1$, $x = 0.5$ and $x = 0.8$. All curves are belonging to ρ_1 and ρ_2 described in Eq. (2.13).

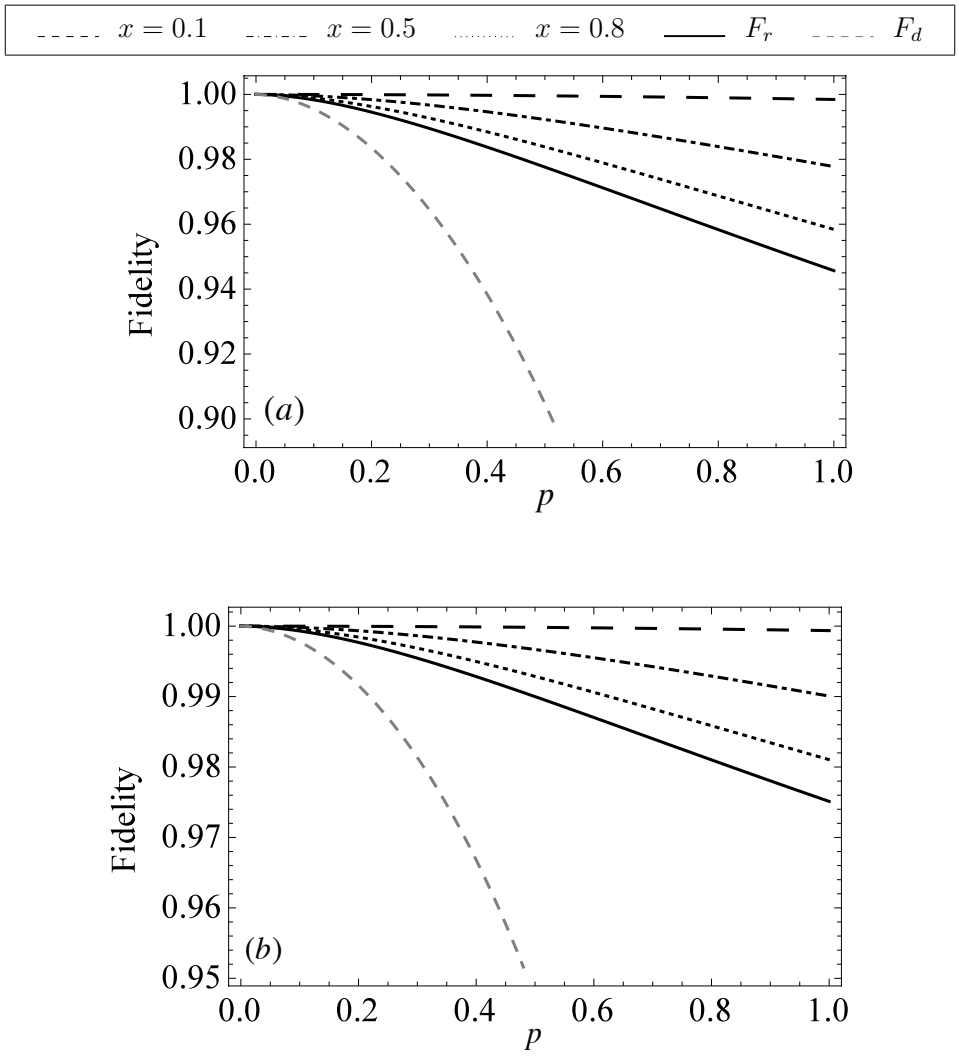

Figure 2.7: Fidelity in the extended scenario as a function of damping probability. Damped state and recovered state corresponds to the results in Section 2.2.1. The other curves relates to $x = 0.1$, $x = 0.5$ and $x = 0.8$ in the extended scenario. All curves are belonging to ρ_1 and ρ_2 described in Eq. (2.13).

3. ROBUST RECOVERY SCHEME

3.1 Robust recovery under uncertainty

In previous chapter, we have considered the scenario where we have the complete knowledge about the parameter of the apparatus. It means that our model would work in the situation where we know the exact values of the parameters, e.g. known p and consequently designing θ based on p. In this situation, as described above, we can follow the reversal scheme outlined in Fig. 2.1 and 2.5, and use them to reverse the initial mixed states when it undergoes amplitude damping.

Another question that has been studied is: *What if we aim to design such an apparatus where we face with some issues of uncertainties?* One of the important issues is uncertainty on p. Furthermore, we know that Hadamard gate angle which works properly for one state may not necessarily be the best one for other states. Below, we depict two scenarios. First, we consider a scenario where we want to design the setup whereas there is a mismatch in the actual p and the one with which we design the angle. We discuss the effect of this mismatching in Sec. 3.1.1. Next, in order to overcome the illustrated shortcoming of this mismatch, we propose a *robust recovery scheme* (RRS) where we can find an optimal Hadamard gate angle and it can be indeed helpful for battling against the uncertainty on p, and also uncertainty around the input state. This approach would be applicable widely, since it requires no initial assumption.

3.1.1 Uncertainty in p

In the previous chapter, we assume that the decay parameter p is known which led to designing θ such that $\theta = \tan^{-1}(1/\sqrt{q})$. However, in practice, one may not have a complete estimate of p, i.e. either completely unknown or known up to an interval.

Therefore, a legitimate question can be *"How can we determine the Hadamard gate angle such that given our uncertainty about p, the achieved fidelity w ould become sufficient?"*

In order to quantify the degrading effect of an unknown p, we conduct a numerical simulation study. Suppose that, we have a point estimation for the value that p can take, say $\hat{p} = 0.7$. Then, based on this value, we set the Hadamard gate angle using $\theta = \tan^{-1}(1/\sqrt{1-p}) = 61.3^o$. Now, we are interested in evaluating the fidelity of this "θ-fixed" recovery scheme across all the possible actual values of p. Moreover, we would like to see the difference in fidelity with the case with known p and adaptive selection of θ as $\theta = \tan^{-1}(1/\sqrt{1-p})$, i.e. for every p design θ such that $\theta = \tan^{-1}(1/\sqrt{1-p})$. Simulation results, for the two mixed density matrices ρ_1 and ρ_2 are shown in Figures 3.1(a) and 3.1(b). We plot the fidelity of recovered scheme by considering fixed θ above (i.e. corresponding to $\hat{p} = 0.7$), along with the two other curves, taken from Figs. 2.2(a) and 2.2(b).

Deducing from Figs. 3.1(a) and 3.1(b), we can summarize the simulation results by the following two points: 1) For fixed $\theta = 61.3^o$, the quantum state is not recovered well on all p's, unless in the range around $p = 0.35$ to 1 for density matrix corresponding to ρ_1 and the range around $p = 0.55$ to 1 for ρ_2. 2) Even though selection of θ through the tangent formula shows a better performance overall, as shown in Figs. 3.1(a) and 3.1(b), one may find a better θ for a specific damped probability p rather than that calculated by $tan^{-1}(1/\sqrt{1-p})$. It seems that in this situation, where we do not know about p, choosing a random p to determine the angle θ is not a considerable way. Hence, in Section 3.1.2, we define a robust method to solve this problem.

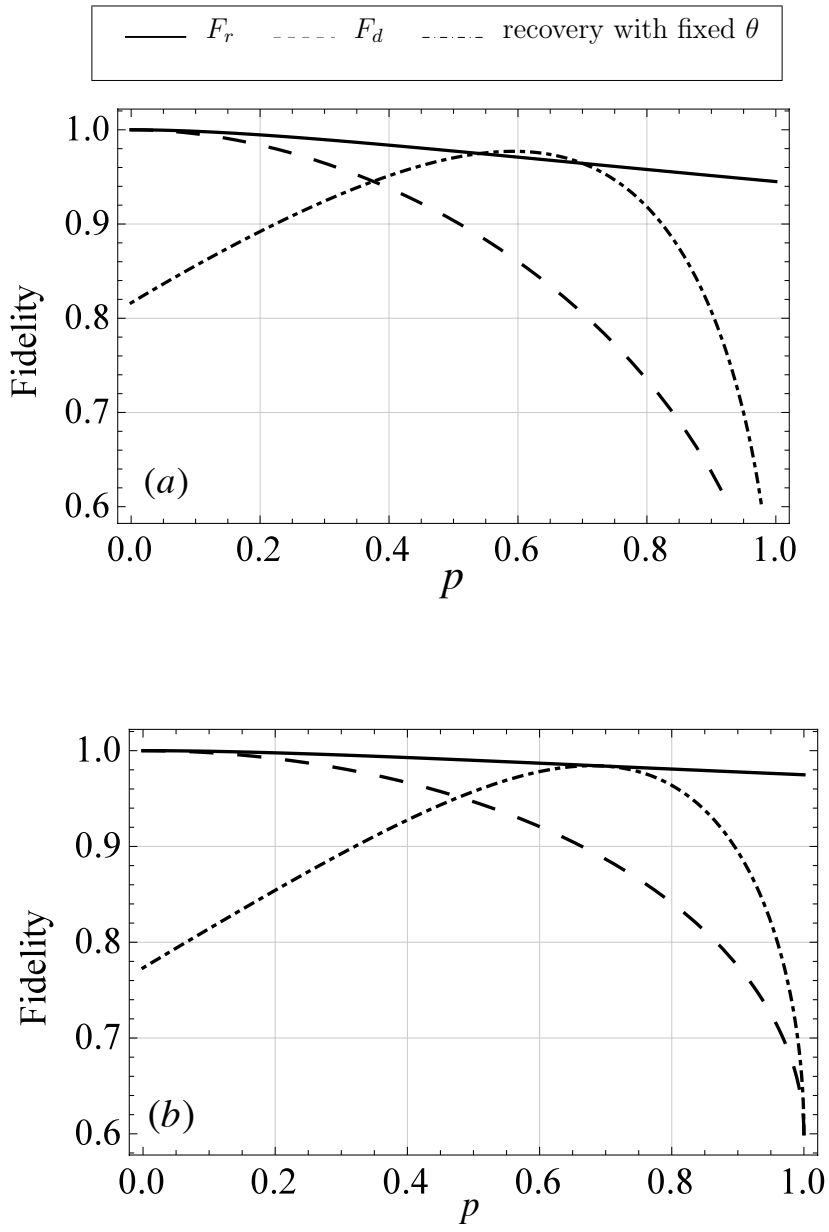

Figure 3.1: The system states are ρ_1 and ρ_2. The solid line and dashed line depends on fidelity with known p and adaptive θ with p, ($\theta = \tan^{-1}(1/\sqrt{1-p})$, used in 2.2.1. The doted line depends on fixed θ which obtains from $\theta = \tan^{-1}(1/\sqrt{0.3})$.

3.1.2 Unknown p and ρ

In the previous subsection, we studied how choosing a Hadamard gate angle θ, where we have uncertainty on p, would affect the fidelity under different values of p. We want now make our uncertainty broader by assuming uncertainty on both p, and the initial quantum state of the system ρ. In this scenario, we introduce a robust recovery scheme based on finding an optimal θ which yields the best average fidelity taken over the distribution.

Definition 1 (Fidelity-Robust Recovery Scheme) *Suppose that the (unknown) density states are governed by a given distribution, i.e., each density matrix has also a probability of occurrence. Then, we define fidelity as a function of ρ, p and θ, and denote it by $F(\rho, p, \theta)$. We define the average fidelity over the range of p and ρ, as follows*

$$\overline{F}(\theta) = E_p \left[E_\rho \left[F(\rho, p, \theta) \right] \right] \tag{3.1}$$

Then, we define a recovery scheme, fidelity-robust, if its Hadamard gate angle θ_{opt} is chosen as follows

$$\theta_{opt} \triangleq \max \overline{F}(\theta). \tag{3.2}$$

We call θ_{opt}, the robust Hadamard gate angle. It should be noted that by averaging we cancel out the roles of unknown ρ and p on the fidelity. This is also called marginalization.

In the case of a given interval, for the (uniformly distributed) unknown $p \in (p_l, p_u)$, we can simplify Eq. (3.1), as follows

$$\overline{F}(\theta) = \frac{1}{p_u - p_l} \int_{p_l}^{p_u} E_\rho \left[F(\rho, p, \theta) \right] dp. \tag{3.3}$$

In many situations, it may not be feasible to find a closed-form solution for either of (3.1) or (3.2). In these cases, one may take numerical approaches for computing the expectations, and solving the maximization problem. In the following, we show an example, where we find the robust angle via Monte Carlo simulations.

To examine the performance of the proposed recovery scheme with the robust angle θ, we compare the case with complete knowledge of θ (the original scheme) with the θ obtained from Eq. (3.2):

$$\overline{F_r} = E_p\Big[E_\rho[F(\rho, p, \theta_p)]\Big], \tag{3.4}$$

where $\theta_p = \tan^{-1}(1/\sqrt{1-p})$.

3.1.3 Simulation

In order to test the RRS scheme and finde the optimal angle, we generate random ρ via Monte Carlo approach with 10^4 iterations, and p also uniformly varies between 0.1 and 0.9. To find the maximum average fidelity, we grid the range of θ between 0 and 2π with steps of $\frac{\pi}{10}$. Fig. 3.2 is depicted these simulation procedures. The results are summarized in Table 3.1. One can find θ_{opt} (among the selected

$F\|\theta$	0	$\pi/10$	$2\pi/10$	$\mathbf{3\pi/10}$	$4\pi/10$	$5\pi/10$	$6\pi/10$	$7\pi/10$	$8\pi/10$	$9\pi/10$	π
$\overline{F}(\theta)$	0.250	0.427	0.632	**0.790**	0.751	0.248	0.090	0.089	0.114	0.154	0.250
$\overline{F_r}$	0.838	0.838	0.838	**0.838**	0.838	0.838	0.838	0.838	0.838	0.838	0.838
$\overline{F_d}$	0.727	0.727	0.727	**0.727**	0.727	0.727	0.727	0.727	0.727	0.727	0.727

Table 3.1: Average recovery fidelity for two scenarios. The first row shows the results for the case where p and ρ are assumed unknown. Also the results are repeated periodically until 2π. The second row show the fidelity for the scenario where the gate angle is chosen with the knowledge of p same as Sec. 2.2.1. The third row is the average damped fidelity.

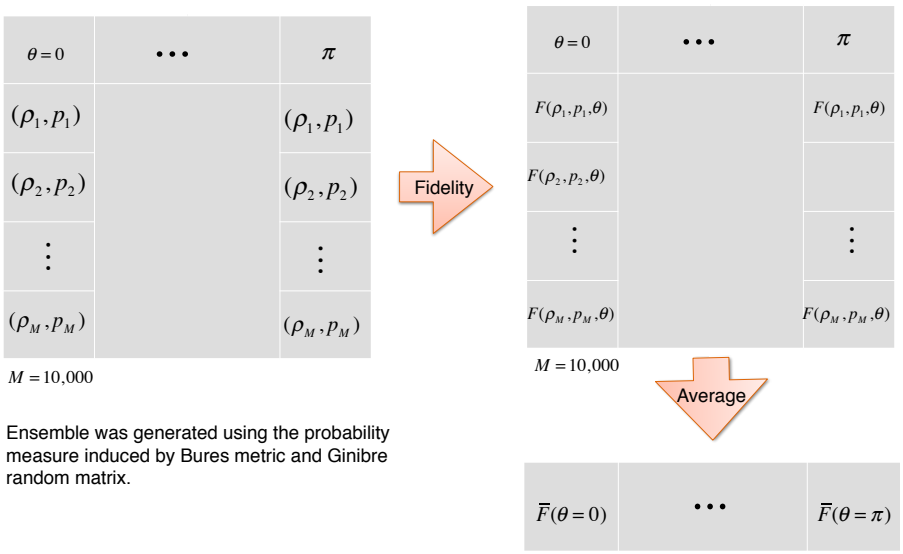

Figure 3.2: The illustrative scheme of Monte Carlo simulations.

candidate angles) by choosing the maximum fidelity among these numbers. The optimal fidelity, bolded in the table, is 0.790 which corresponds to $3\pi/10$. We omit the rest of numbers after π, because they periodically repeat. Although 0.790 is smaller than the fidelity 0.838 in the case we have know exactly what the p is, it is still larger than the damped fidelity 0.727. One should note that, one may achieve better results by a finer grid of θ. Next, we test the idea by choosing the probability of decay in the case of smaler range than previous consideration where it was varied from 0.4 to 0.6 and also from 0.45 to 0.55. The results showed in the table 3.2 and 3.3.

As we expected, the simulation results show that when the the interval is tight enough, i.e. low amount of uncertainty meaning being closer to the complete information situation, we can achieve near-optimal results. Overall, one may conclude that via the robust recovery scheme, the mixed states recovery can be robustly im-

$F\|\theta$	0	$\pi/10$	$2\pi/10$	$\mathbf{3\pi/10}$	$4\pi/10$	$5\pi/10$	$6\pi/10$	$7\pi/10$	$8\pi/10$	$9\pi/10$	π
$\overline{F}(\theta)$	0.2497	0.4268	0.6348	**0.7967**	0.7487	0.2500	0.0883	0.0885	0.1091	0.1566	0.2497
$\overline{F_r}$	0.8345	0.8345	0.8345	**0.8345**	0.8345	0.8345	0.8345	0.8345	0.8345	0.8345	0.8345
$\overline{F_d}$	0.7409	0.7409	0.7409	**0.7409**	0.7409	0.7409	0.7409	0.7409	0.7409	0.7409	0.7409

Table 3.2: Average recovery fidelity for two scenarios. p varied from 0.40 to 0.60. The first row shows the results for the RRS scheme. The second row show the fidelity for the scenario where the gate angle is chosen with the knowledge of p same as Sec. 2.2.1. The third row is the average damped fidelity.

$F\|\theta$	0	$\pi/10$	$2\pi/10$	$\mathbf{3\pi/10}$	$4\pi/10$	$5\pi/10$	$6\pi/10$	$7\pi/10$	$8\pi/10$	$9\pi/10$	π
$\overline{F}(\theta)$	0.2498	0.4274	0.6362	**0.7987**	0.7507	0.2506	0.0922	0.0917	0.1091	0.1577	0.2498
$\overline{F_r}$	0.8362	0.8362	0.8362	**0.8362**	0.8362	0.8362	0.8362	0.8362	0.8362	0.8362	0.8362
$\overline{F_d}$	0.7438	0.7438	0.7438	**0.7438**	0.7438	0.7438	0.7438	0.7438	0.7438	0.7438	0.7438

Table 3.3: Average recovery fidelity for two scenarios. p varied from 0.45 to 0.55. The first row shows the results for the RRS scheme. The second row shows the fidelity for the scenario where the gate angle is chosen with the knowledge of p same as Sec. 2.2.1. The third row is the average damped fidelity.

plemented with no (or limited) knowledge of the underlying p or ρ, and one would need to quantify the prior knowledge in the form of distributions governing these two variables. This is of high importance given the fact that in practice, one may only have limited knowledge regarding the quantum system parameters.

4. CONCLUSION

In summary this thesis presented variety approaches in order to protect an arbitrary two qubit mixed state from amplitude damping. Starting from reviewing recovery of quantum states from amplitude damping in the weak measurement framework. In the second step, we reported recovery schemes without considering weak measurement in the mixed state framework where mixed state involves many more parameters than the pure state and it is mathematically many complicated. The basic scheme without preparation stage can recover a quantum state with very high fidelity, but the quantum entanglement of the two-qubit mixed state is not significantly improved. The extended scheme with preparation stage can recover the two-qubit mixed state with a very high fidelity and the quantum entanglement can be also significantly recovered by choosing suitable parameters. Furthermore, the extended scheme can also recover a quantum state even beyond the ESD point.

In addition, a recovery scheme was next introduced which takes the system's uncertainties into account which in turn led to a robust recovery scheme. Firs we studied the effect of choosing inappropriate decay probability where we have partial knowledge about the parameter of the apparatus in order to design our recovery scheme. We saw this mismatch had not appropriate results for variety of apparatus with different decay probabilities. Then we proposed “Robust Recovery" method where not only we had partial knowledge about decay probability, but also we had uncertainty in the initial state. We find an optimal angle for recovering a two-qubit mixed state when the quantum state and the decay probability were unknown. This scheme may be very useful for protecting a quantum state from amplitude damping in practice.

REFERENCES

[1] Lidar D A, Chuang I L and Whaley K B 1998 *Phys. Rev. Lett.* **81** 2594

[2] Shor P W 1995 *Phys. Rev. A* **52** R2493

[3] Duan L M and Guo G C 1997 *Phys. Rev. Lett.* **79** 1953

[4] Facchi P, Lidar D and Pascazio S 2004 *Phys. Rev. A* **69** 032314

[5] Maniscalco S, Francica F, Zaffino R L, Gullo N L and Plastina F 2008 *Phys. Rev Lett.* **100** 090503

[6] Viola L and Lloyd S 1998 *Phys. Rev. A* **58** 2733

[7] Viola L, Knill E and Lloyd S 1999 *Phys. Rev. Lett.* **82** 2417

[8] Weisskopf V F and Wigner E P 1930 *Z. Phys.* **63** 54–73

[9] Preskill, John. "Lecture notes for physics 229: Quantum information and computation." California Institute of Technology (1998): 16.

[10] Nielsen, Michael A., and Isaac L. Chuang. Quantum computation and quantum information. Cambridge university press, 2010.

[11] Katz N., Nadav, Ansmann M., Bialczak Radoslaw C. , Erik L., McDermott R., Neeley M. , Steffen M., Weig E. M., Cleland A. N. , Andrew M. M., Korotkov A. N.

[12] Sun Q, Al-Amri M, Davidovich L and Zubairy M S 2010 *Phys. Rev. A* **82** 052323

[13] Korotkov A N and Jordan A N 2006 *Phys. Rev. Lett.* **97** 166805

[14] Sun Q, Al-Amri M and Zubairy M S 2009 *Phys. Rev. A* **80** 033838

[15] Kim Y S, Lee J C, Kwon O and Kim Y H 2012 *Nature Phys.* **8** 117–120

[16] Korotkov A N and Keane K 2010 *Phys. Rev. A* **81** 040103

[17] Al Amri M, Scully M O and Zubairy M S 2011 *J. Phys. B: At. Mol. Opt. Phys.* **44** 165509

[18] Liao Z, Al-Amri M and Zubairy M S 2013 *J. Phys. B: At. Mol. Opt. Phys.* **46** 145501

[19] Rauschenbeutel A, Nogues G, Osnaghi S, Bertet P, Brune M, Raimond J and Haroche S 1999 *Phys. Rev. Lett.* **83** 5166

[20] Jozsa R 1994 *J. mod. opt.* **41** 2315–2323

[21] Miszczak J A 2012 *Com. Phys. Comm.* **183** 118–124

[22] Życzkowski K, Penson K A, Nechita I and Collins B 2011 *J. Math. Phys.* **52** 062201

[23] Mezzadri F 2006 *arXiv preprint math-ph/0609050*

[24] Wootters W K 1998 *Phys. Rev. Lett.* **80** 2245

[25] Tahira R, Ikram M, Azim T and Zubairy M S 2008 *J. Phys. B: Atom, Mol. Opt. Phys.* **41** 205501

[26] Yu T and Eberly J 2006 *Opt. Comm.* **264** 393–397